Expanded View Figures

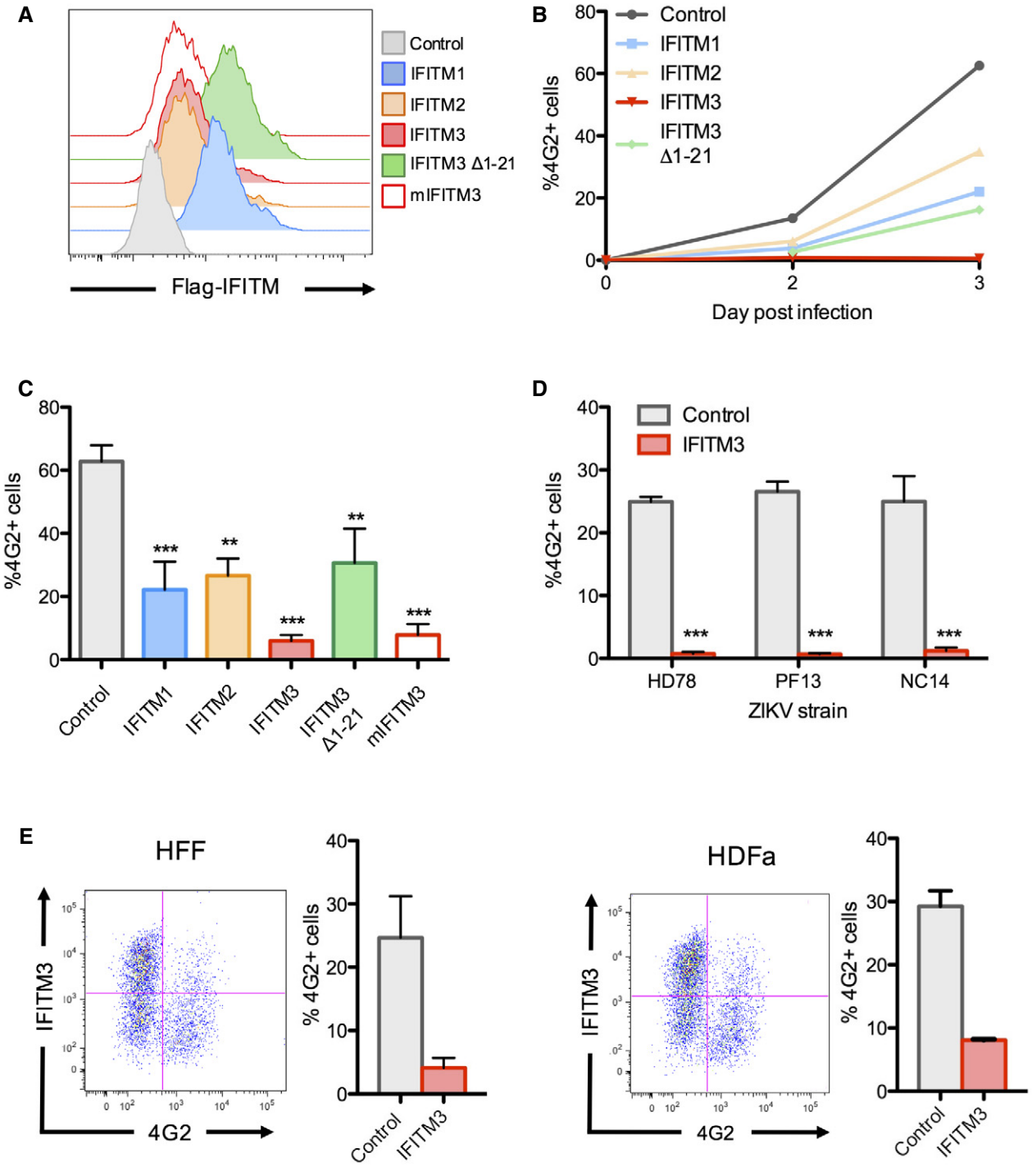

Figure EV1.

Figure EV1. Expression of IFITMs in 293T cells and human primary fibroblasts restricts ZIKV replication.

A Stable IFITM-positive cell lines were produced in 293T cells, and the expression of each protein was measured by flow cytometry.

B 293T cells were infected with ZIKV HD78 (MOI 1), and viral replication was measured at days 2 and 3 post-infection (pi) by flow cytometry using the anti-E protein antibody 4G2, as illustrated in one representative experiment.

C Results from four independent experiments as in (B) were quantified at day 3 pi. Mean ± SEM.

D 293T cells expressing or not IFITM3 were infected with the indicated ZIKV strains. Viral replication was measured at day 2 or 3 post-infection (pi) by flow cytometry using the anti-E protein antibody 4G2. Results are mean ± SEM of three independent experiments.

E Human foreskin fibroblasts (HFF) (left panels) or human adult dermal fibroblasts (HDFa) (right panels) overexpressing or not IFITM3 were infected with ZIKV, and the % of E-positive cells was measured by flow cytometry at day 2 pi. For each cell type, one representative experiment is shown on the left and the mean ± SEM of three independent experiments on the right.

Data information: Statistical significance was determined using ANOVA test. ***$P < 0.001$; **$P < 0.01$.

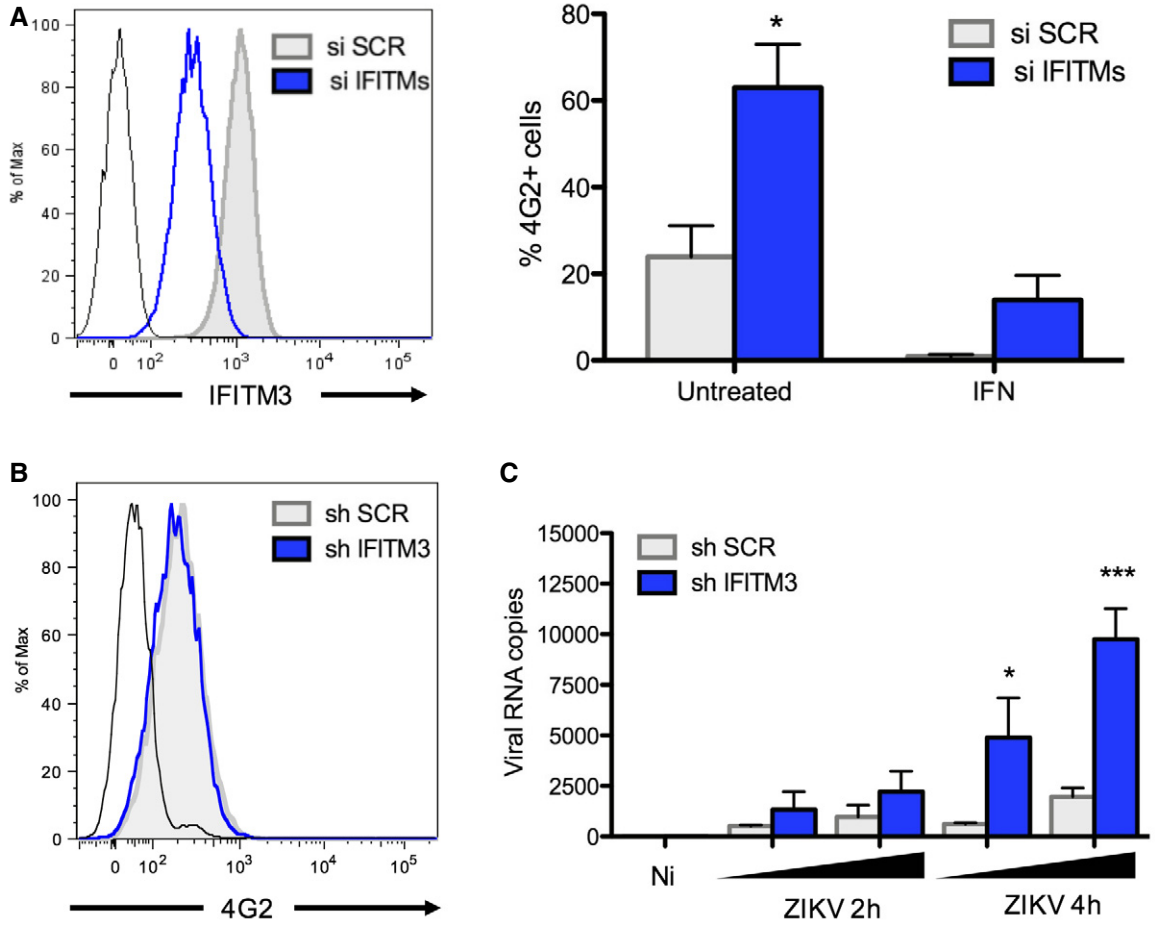

Figure EV2. Endogenous IFITM3 protein inhibits ZIKV replication at an early stage.

A Effect of IFITM3 in HDFa cells. Left panel: The levels of endogenous IFITM3 were assessed by flow cytometry in HDFa transfected with a control siRNA or siRNA targeting IFITM3. Black curve: isotype control. Right panel: The cells were pretreated or not with IFN-α (1,000 IU/ml for 48 h) and infected with ZIKV HD78 (MOI 1) for 24 h. Infected cells were scored by 4G2 staining and flow cytometry (right panel). Mean ± SEM from three independent experiments is shown.

B IFITM3 does not affect virus attachment to target cells. HeLa sh-SCR or sh-IFITM3 were incubated with ZIKV for 1 h at 4°C. The mean fluorescence intensity (MFI) of 4G2 staining was determined by flow cytometry. Black curve: isotype control.

C IFITM3 prevents intracellular accumulation of viral RNA. HeLa sh-SCR or sh-IFITM3 were infected with ZIKV for 2 or 4 h at 37°C. The black triangle indicates increasing amounts of virus (MOI 3 and 10). Virus remaining at the cell surface was removed by trypsin treatment. The cellular RNA was extracted, and RT-qPCR was performed to quantify viral RNA. Mean ± SEM of three independent experiments.

Data information: Statistical significance was determined using ANOVA test and Bonferroni post-test. ***$P < 0.001$; *$P < 0.05$.

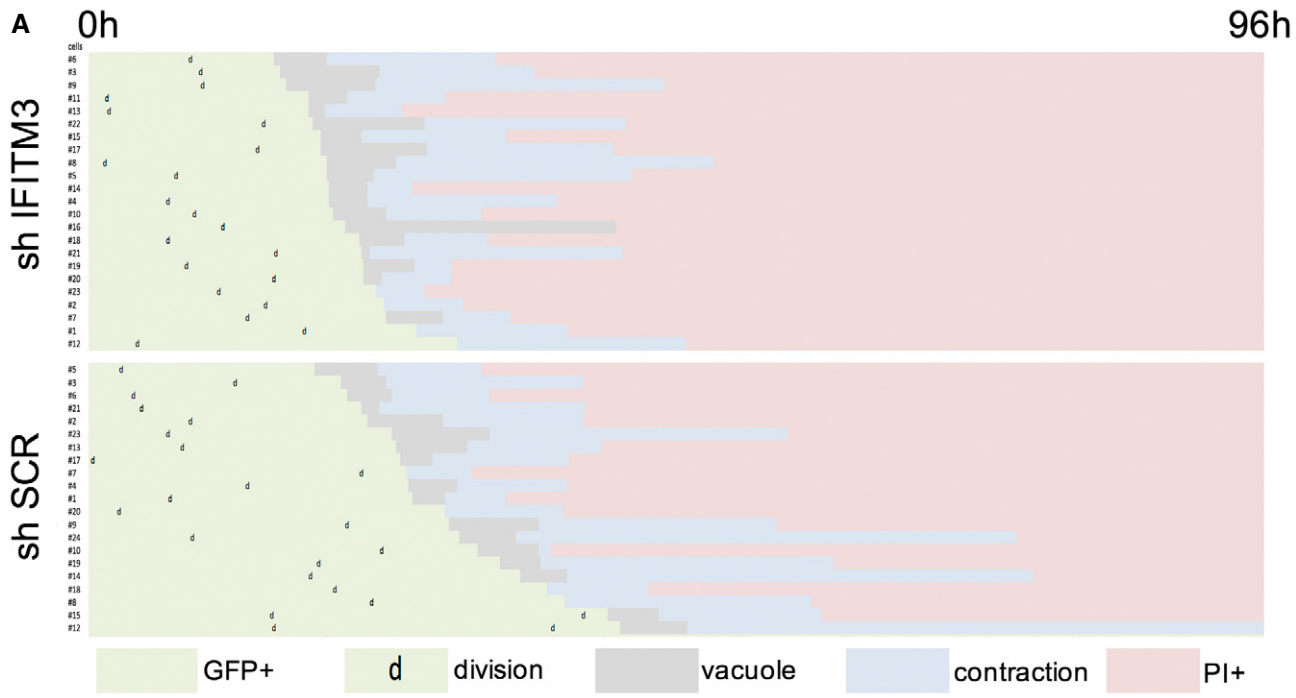

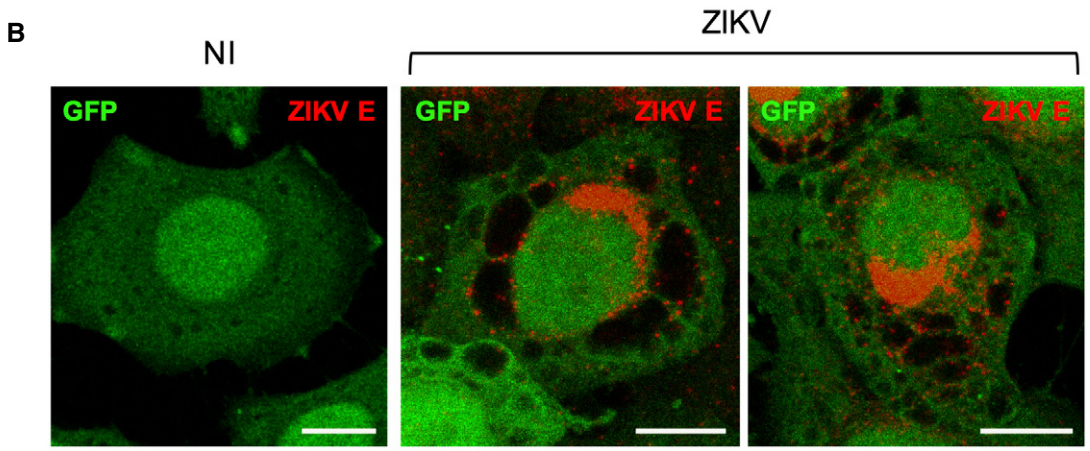

Figure EV3. ZIKV-induced cytoplasmic vacuolization and cytopathic effects.

A Time-lapse analysis of the morphological changes observed in ZIKV-infected cells. HeLa sh-SCR and HeLa sh-IFITM3 cells were infected with ZIKV HD78 (MOI 1) and recorded using time-lapse microscopy. For each condition, about 20 individual cells that end up dying upon ZIKV infection were selected for further analysis. Morphological changes were visually scored for each cell. Results are representative of three independent experiments.

B HeLa sh-SCR cells were infected or not with ZIKV HD78 (MOI 1) for 24 h, fixed, and stained to detect ZIKV E protein (red). One single Z slice representative of three independent experiments is shown. Scale bars: 5 μm.

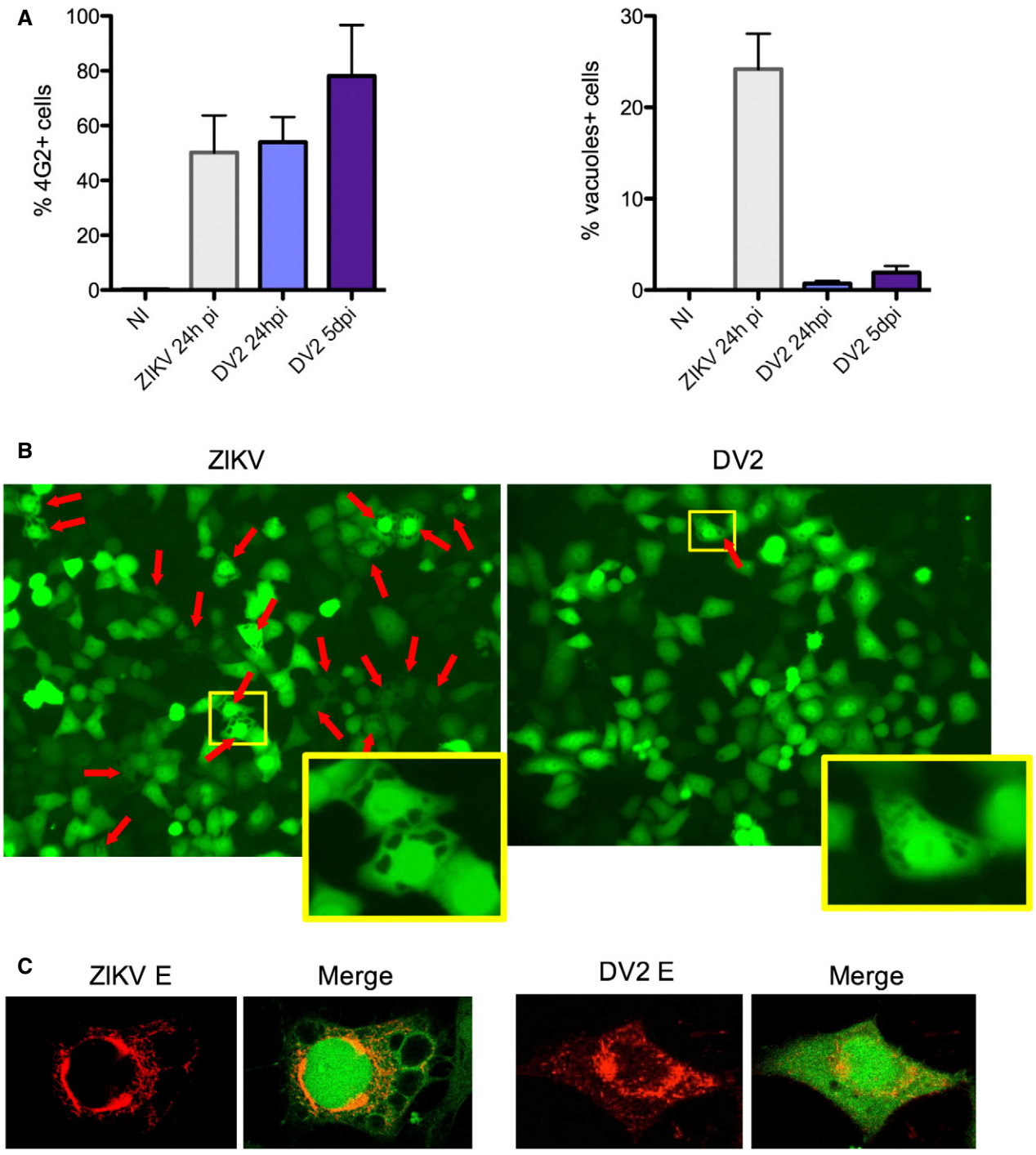

Figure EV4. Morphological changes induced by ZIKV HD78 and DENV2.

A HeLa sh-IFITM3 were infected with ZIKV HD78 or DV2 for 24 h or 5 days pi. Left panel: The levels of infection were determined by 4G2 staining and flow cytometry. Right panel: The proportion of cells displaying vacuoles was scored by visual examination of at least 200 cells at 24 h pi (right panel). Mean ± SEM of three independent experiments.

B One example of a representative field from (A) is shown for ZIKV (left) and DENV2 (right) infected cells at 24 h pi. Red arrows point to vacuole$^+$ cells. For each condition, an enlarged view of a vacuolated cell is shown.

C Examples of ZIKV- and DENV-infected cells, with 4G2 staining and confocal microscopy analysis.

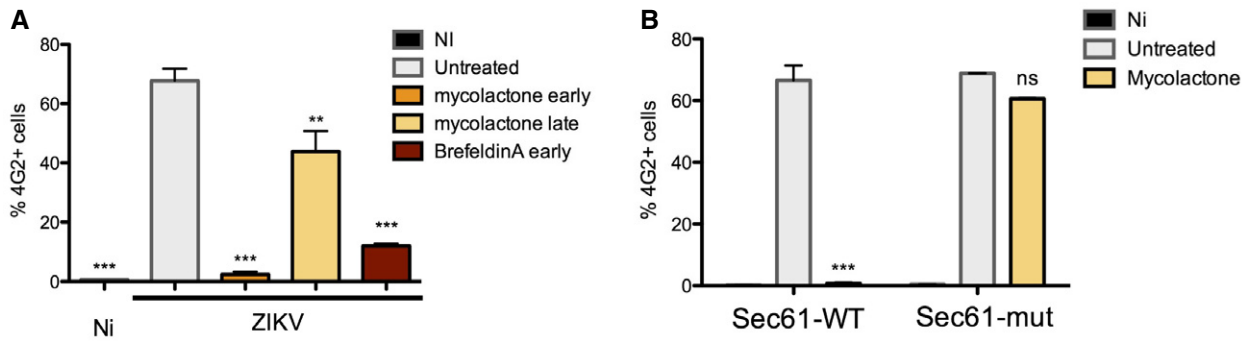

Figure EV5. Effect of mycolactone on ZIKV replication.

A HeLa sh-IFITM3 were infected with ZIKV HD 78 (MOI 1) for 24 h in the presence or absence of mycolactone (20 nM) added at 2 h (mycolactone early) or 15 h pi (mycolactone late). Brefeldin A (0.5 μg/ml) was added during the 24 h of infection. The levels of infection were determined by 4G2 staining and flow cytometry. Results are mean ± SEM of three independent infections.

B 293T cells expressing WT Sec61 or a mutated Sec61 resistant to mycolactone (Sec61-mut) were infected with ZIKV HD 78 (MOI 1) for 3 days in the presence or absence of mycolactone (20 nM). The levels of infection were determined by 4G2 staining and flow cytometry. Results are mean ± SEM of three independent infections.

Data information: Statistical significance was determined using ANOVA and Bonferroni post-tests. ***$P < 0.001$; **$P < 0.01$; ns, $P > 0.05$.

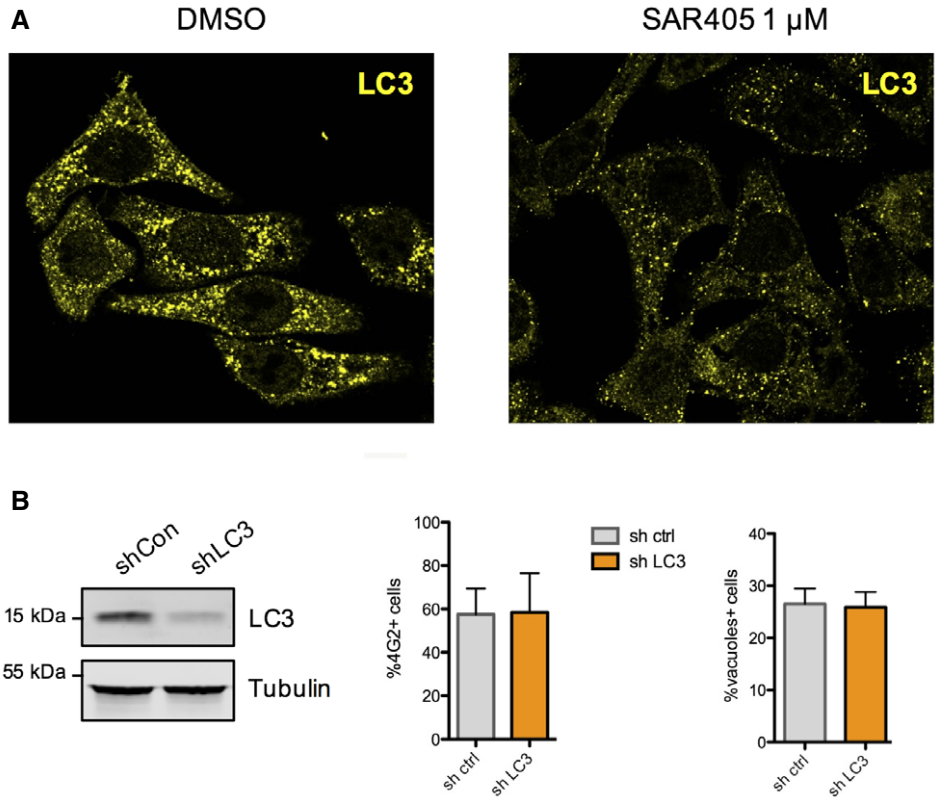

Figure EV6. Impact of LC3 on ZIKV-induced vacuole formation.

A The class 1 PI3K inhibitor blocks autophagy assessed by LC3 clustering in HeLa sh-IFITM3 treated with rapamycin (5 mM) and concanamycin A (1 μM), which prevents fusion of phagosomes with lysosomes.

B HeLa cells expressing a shRNA control or a shRNA targeting LC3 were infected with ZIKV HD78 (moi 1) for 24 h, and the % of E^+ cells as well as the % of vacuole-containing cells were quantified by flow cytometry and microscopy, respectively. The efficiency of silencing was assessed by Western blot (left panel). Results are shown as mean ± SEM from three independent experiments.